

# Athermal design of nearly incompressible bonds

Keith B. Doyle

Optical Research Associates, 1800 West Park Drive, Westborough, MA

Gregory J. Michels, Victor L. Genberg  
Sigmadyne, Inc., Rochester, NY

## ABSTRACT

Selecting the proper thickness of high shape factor bonds using near incompressible adhesives is critical to minimize the elastic response of the bonded optical element. For incompressible adhesives with low shape factor, variations in the bond thickness are shown not to be as critical. This is illustrated in the evaluation and redesign of an RTV bond for a primary mirror of a Cassegrain telescope. The initial bond was oversized and highly constrained resulting in focus errors in the telescope during optical testing. Subsequent redesign of the bond thickness to athermalize the design compared various closed-form solutions and finite element parametric studies.

**Keywords:** adhesives, constrained bonds, thin bonds, optical mounting, RTV, finite element analysis, athermal

## 1. BEHAVIOR OF NEARLY INCOMPRESSIBLE MATERIALS

Rubber and rubber-like materials such as RTV are nearly incompressible. Incompressibility is characterized by a Poisson ratio approaching 0.5 and a bulk modulus tending to infinity. Bulk modulus is defined as the relative ability of a material to maintain constant volume under load. It is computed as the ratio of the hydrostatic compressive stress to the decrease in volume. The relationship between the bulk modulus,  $B$ , and Poisson ratio,  $\nu$ , is given by equation 1.1.

$$B = \frac{E}{3(1-2\nu)} \quad (1.1)$$

For bonds that are characterized by a high shape factor (ratio of the loaded area to the force free area), which is characteristic of thin bonds and/or a mounting geometry that constrains bond deformation, significant forces may be imparted to the optical element due to the effective stiffness of the bond material. Finite-element derived and closed-form equations exist for common bond shapes that relate the compressive stiffness in the direction of the load to the space available for the RTV to deform<sup>1</sup>. The compressive stiffness is often referred to as the compressive modulus. However, the compressive stiffness is not a material property as implied by the modulus term, but a term in the Hooke's stiffness matrix relating stress and strain. For nearly incompressible bonds with a high shape factor, the value of the compressive stiffness approaches the bulk modulus. In these instances, proper selection of bond thickness is critical in minimizing forces applied to the optical element.

## 2. RTV DESIGN EXAMPLE

An afocal telescope, which acts as a beam expander in a sensing system, experienced focus shifts that exceeded the allowable due to uniform changes in the ambient temperature. A schematic of

the primary mirror assembly is shown in Figure 1.a. The 6.3-inch diameter mirror with a front radius of curvature of 25-inches is bonded to a stainless steel 416 bezel using a 0.1-inch full circumferential ring bond made of GE RTV630. In the nominal design, the RTV bond contacts both the front lip of the bezel and the primary mirror as shown in Figure 1.b. This was done to minimize axial spacing changes between the primary and secondary mirror under the operational environment that includes inertial and dynamic loads acting at various telescope orientations over uniform temperature changes.

During optical testing, the telescope assembly experienced greater than expected focus errors over uniform temperature changes. The on-axis telescope wavefront error was measured as a function of temperature using a LUPI interferometer. The dominant Zernike polynomial term representing the wavefront error is focus. Peak-to-valley focus error is plotted as a function of temperature in Figure 2 and listed in Table 1. The focus error is approximately linear with temperature. The slope of the data represents the focus error sensitivity of 0.19  $\mu\text{m}/\text{C}$ .

Optical Test Data: WFE ( $\mu\text{m}$ )			
$\Delta T$ (C)	RMS	P-V	P-V Focus
0.7	0.035	0.149	0.134
1.5	0.074	0.320	0.286
2.0	0.100	0.426	0.382
2.7	0.135	0.575	0.516
3.2	0.162	0.682	0.611
3.8	0.188	0.809	0.726

Table 1. On-Axis Optical Test Data

### 3. OPTICAL ANALYSIS

A series of analyses were undertaken to determine the cause of the focus error in the telescope. One hypothesis theorized that the radius of curvature of the primary mirror was changing due to mount-induced deformation. A sensitivity analysis was conducted using a CODE V optical model of the test setup to compute the wavefront due to a change in the radius of curvature of the primary mirror. For an edge-mounted mirror, a radius of curvature change is accompanied by an axial repositioning or despace of the vertex of the primary. (This effect was included but proved to be insignificant). The sensitivity analysis resulted in a 0.0176 P-V focus error per  $\mu\text{m}$  change in the radius of curvature of the primary mirror.

WFE P-V Focus Error ( $\mu\text{m}/\text{C}$ )	
Test Data	0.190
CODE V	0.170

Table 2. WFE Focus Error Comparison of Optical Test Data to Optical Model Data

Thus to achieve the P-V wavefront error of 0.19  $\mu\text{m}/\text{C}$  measured during optical testing, a 10.8  $\mu\text{m}$  change in the radius of curvature of the primary mirror would have to result for a one degree C change in temperature. To check this, a 10.8  $\mu\text{m}$  change in the radius of curvature of the primary mirror was imposed in the optical model. This produced a peak-to-valley focus error of 0.17  $\mu\text{m}$ . A comparison of the optical test data and the optical model are given in Table 2. The differences are relatively small, suggesting that the source of the wavefront error is indeed a change in the radius of curvature of the primary mirror. For reference, these wavefront errors far exceeded the allowable focus change of the primary mirror of 0.023  $\mu\text{m}/\text{C}$ .

#### 4. MECHANICAL ANALYSIS

A finite element model was created of the primary mirror assembly to evaluate the change in the shape of the primary mirror for a uniform increase in temperature. Views of the finite element model are shown in Figure 3. Mechanical properties as supplied by the manufacturer for the GE RTV630 include a Shore A durometer hardness of 60, and a coefficient of thermal expansion of 210 ppm/C. As noted above, the elastic response of the optical mount is highly dependent upon the value of Poisson ratio, which is typically not supplied by the manufacturer. One method to approximate the Poisson ratio is to use the material data for rubber published by Lindley<sup>2</sup>. Lindley lists the elastic and bulk modulus for various Shore A durometer hardness values. For a Shore A durometer hardness of 60, an elastic modulus of 645 psi and a bulk modulus of 166 ksi are given. Using equation 1.1, a Poisson ratio of 0.49935 is computed. The material properties used in the finite element model are listed in Table 3.

Material Properties			
	E (psi)	$\nu$	CTE (ppm/C)
ULE	9.8e6	0.176	0.03
RTV	645	0.49935	210
SS416	29.e6	0.28	9.9

Table 3. Material Properties used in the Finite Element Analysis

A finite element analysis was performed to compute the best-fit radius of curvature change for a one-degree C change in the ambient temperature. The optical surface deformations were read into the optomechanical analysis software package *SigFit*<sup>3</sup> for Zernike polynomial fitting. The best-fit radius of curvature change was then computed using the Zernike focus term. The results indicated that for a one degree C change in temperature, the change in the radius of curvature is 18.8  $\mu\text{m}/\text{C}$ . This compares to the backed out value of 10.8  $\mu\text{m}/\text{C}$  change in the radius of curvature from the optical test data. Thus, it was concluded that the nominal RTV bond was improperly sized and was exerting forces on the primary mirror resulting in radius of curvature changes.

A study was then performed to compare the change in radius of curvature as a function of Poisson ratio. Using values of Poisson ratio for RTV from 0.4 to 0.4999, the change in radius of curvature ranges from 0.9 to 20.7  $\mu\text{m}/\text{C}$ . The results are displayed in Figure 4 and illustrate the critical role Poisson ratio plays in the elastic response of bonded optical elements.

#### 5. BOND THICKNESS: ATHERMAL DESIGN EQUATIONS

The RTV bond was redesigned to minimize/eliminate radius of curvature changes of the primary mirror. After considering other influences, the redesign effort was simplified by considering only uniform temperature changes as part of the operational environment. This eliminates the need to constrain axial motion of the primary mirror and a simple ring shape (as shown in Figure 5) or discrete bond pads can be considered. As will be shown, properly sizing the thickness of high shape factor RTV bonds is critical. A comparison of closed-form solutions for athermal sizing of the bond thickness was performed and compared to the finite element computed athermal thickness.

## Closed-Form Solutions

The first closed-form equation considered can be derived based on elementary considerations (i.e. bond expansion/contraction equals the difference in radial growth of the lens cell and the optical element), and is given by<sup>4</sup>:

$$t_{bond} = r_{optic} \frac{\alpha_{cell} - \alpha_{optic}}{\alpha_{bond}^* - \alpha_{cell}} \quad (5.1)$$

Proper use of this equation for high Poisson ratio materials, requires that the effective CTE,  $\alpha_{bond}^*$ , of the adhesive material be used<sup>5</sup>. This effective CTE value is a function of the bond and mounting geometry and may be computed using curves from Michels<sup>1</sup>. Computing the bond thickness using equation 5.1 requires several iterations since the effective CTE is based on the thickness of the bond.

Deluzio<sup>6</sup> presents an equation to athermally size adhesive bonds expressed in equation 5.2.

$$t_{bond} = r_{optic} \frac{(1 - \nu_{bond})}{(1 + \nu_{bond})} \left[ \frac{\alpha_{cell} - \alpha_{optic}}{(\alpha_{bond} - \alpha_{optic}) - \frac{(7 - 6\nu_{bond})(\alpha_{cell} - \alpha_{optic})}{4(1 + \nu_{bond})}} \right] \quad (5.2)$$

For materials where the Poisson ratio approaches 0.5, the above equation simplifies to

$$t_{bond} = r_{optic} \frac{\alpha_{cell} - \alpha_{optic}}{3\alpha_{bond} - 2\alpha_{cell} - \alpha_{optic}} \quad (5.3)$$

Meunch<sup>7</sup> presents an equation to compute an optimum bond thickness in equation 5.4.

$$t_{bond} = r_{optic} \frac{(1 - \nu_{bond})(\alpha_{cell} - \alpha_{optic})}{\alpha_{bond} - \alpha_{cell} + \nu_{bond}(\alpha_{bond} - \alpha_{optic})} \quad (5.4)$$

This equation assumes a Poisson ratio of 0.43 for the bond adhesive.

The athermal bond thickness computed using the above three approaches are listed in Table 4. An effective CTE of 620 ppm/C was used in equation 5.1.

Athermal Bond Thickness	
Equation	t (mm)
Bayer	1.30
Deluzio	1.30
Muench	1.55

Table 4. Athermal Bond Thickness Comparison

## FEA Parametric Evaluation

A finite element model of the telescope's primary mirror, RTV elastomer, and bezel was created. The model was used to parametrically evaluate the change in the radius of curvature of the primary mirror as a function of bond thickness for a unit C change in temperature. The RTV was modeled with an elastic modulus of 645 psi, a CTE of 210 ppm/°C, and a Poisson's ratio of 0.49935. A plot of RTV bond thickness versus change in radius of curvature is shown in Figure 6. The athermal bond thickness, where there is no change in the radius of curvature of the mirror, is the same value as that predicted by Bayer's modified and Deluzio's equation - 1.30 mm. Meunch's equation produces a radius of curvature change of 6.2  $\mu\text{m}/\text{C}$  - corresponding to a 0.11  $\mu\text{m}$  p-v focus error. For comparison purposes, the radius of curvature change of the mirror if unconstrained is 0.02  $\mu\text{m}/\text{C}$ . For the case where the RTV bond line goes to zero, and the mirror is hard-mounted against the bezel the radius of curvature change is 81  $\mu\text{m}/\text{C}$ .

Sizing the thickness of the full circumferential ring bond is critical in minimizing radius of curvature changes in the primary mirror as illustrated in Figure 6. Variations in the athermal thickness result in significant changes in the radius of curvature. This is a result of the high shape factor of the bond, which yields a compressive stiffness nearing the bulk modulus. To compare the sensitivity of the bond thickness as a function of shape factor, a study was performed to compute changes in the radius of curvature as a function of bond thickness using a bond made of discrete pads. Thirty-six discrete pads were used to hold the primary mirror in the bezel. The shape factor varied from 1 to 4 as the thickness was varied from 2.54 mm to 0.635 mm. For RTV bonds with a low shape factor, the compressive stiffness is greatly reduced and is near the elastic modulus. (For comparison, the shape factor for the ring bond varied from 10 to 40). The plot of radius of curvature variation for both cases is plotted in Figure 7. Notice how the variation in thickness is not critical for low shape factor designs.

## **SUMMARY**

Due to the near incompressibility of RTV, care must be taken in the design of RTV bonds with high shape factors. This is illustrated in the evaluation and redesign of a RTV bond for the primary mirror of a Cassegrain telescope. The initial design was oversized and highly constrained resulting in focus errors in the telescope during optical testing. Subsequent redesign of the bond thickness using closed-form equations and finite element parametric studies resulted in an athermal design. For adhesives that do not have a Poisson ratio near 0.5 or have a low shape factor, variations in the thickness of the bond are not as critical. Using Bayer's equation with an effective CTE yields an athermal bond thickness. This is verified by Deluzio's equation using a nominal CTE value.

## **ACKNOWLEDGMENTS**

The authors would like to acknowledge Mark Kahan of Optical Research Associates, Marc Daigle from Optical Alchemy, and Robert Fata of the Smithsonian Astrophysical Observatory.

## **REFERENCES**

<sup>1</sup>Michels, G. J., Genberg, V. L., Doyle, K. B., "Finite element modeling of nearly incompressible bonds", Proc. SPIE 4771 (34), July, 2002.

<sup>2</sup>Lindley, P. B., “Engineering Design with Natural Rubber”, Natural Rubber Technical Bulletin, 3<sup>rd</sup> Edition, published by the National Rubber Producers Research Association, 1970.

<sup>3</sup>*SigFit* is written by Sigmadyne, Inc., Rochester, NY

<sup>4</sup>Bayar, M., “Lens barrel optomechanical principles”, Optical Engineering, Vol. 20, No. 2, 181 (March/April 1981).

<sup>5</sup>Fata, R. G., Fabricant, D., “Design of a cell for the wide-field corrector for the converted MMT”, Proc. SPIE 1998, 32 1993.

<sup>6</sup>Deluzio, "Optimization of elastomer thickness for edge mounted mirrors subject to uniform temperature changes".

<sup>7</sup>Vukobratovich, D, et al., “Bonded mounts for small cryogenic optics”, Proc. SPIE 4131, 2000.

### Figures

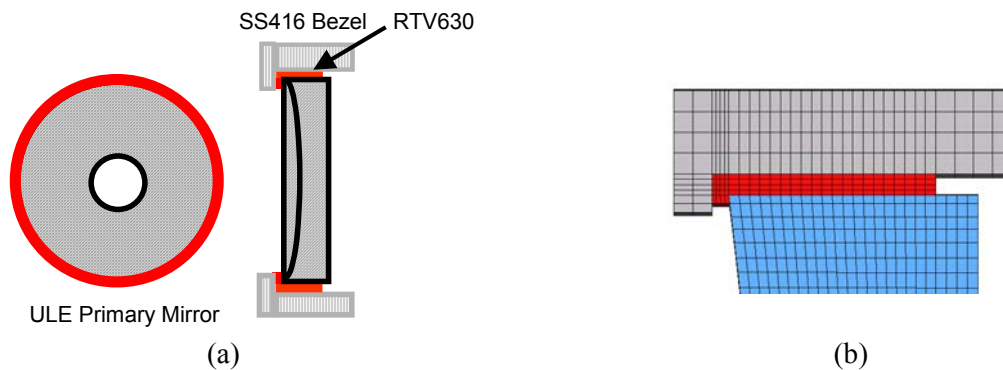


Figure 1. Cassegrain Telescope Schematic a) full circumferential ring bond; b) close-up view showing RTV contacting front lip of bezel and primary mirror

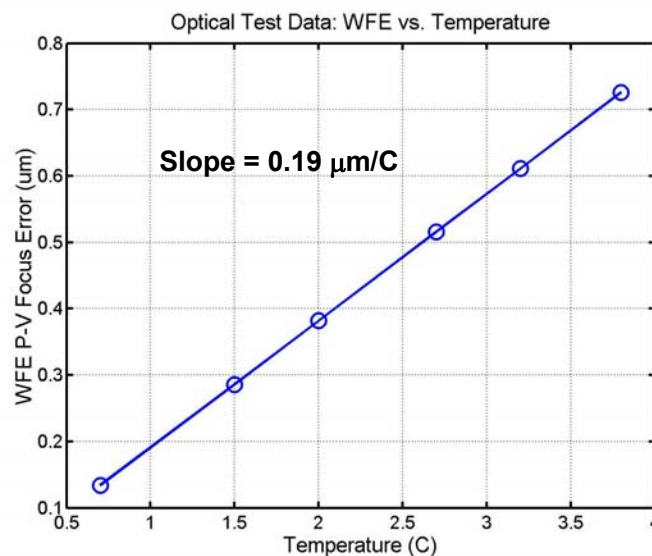


Figure 2. Optical Test Results: P-V Wavefront Error vs. Ambient Temperature Changes

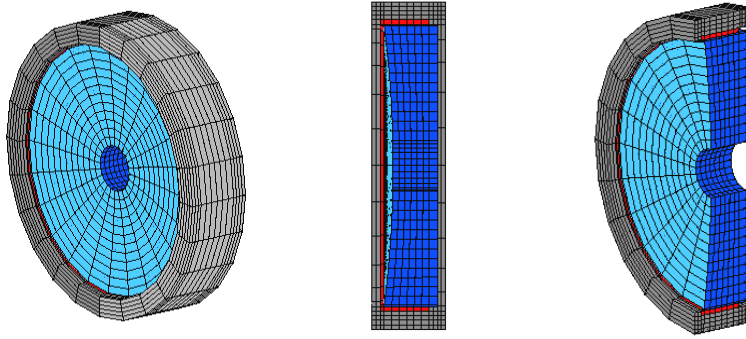


Figure 3. Views of Finite Element Model: Primary Mirror, RTV, & Bezel

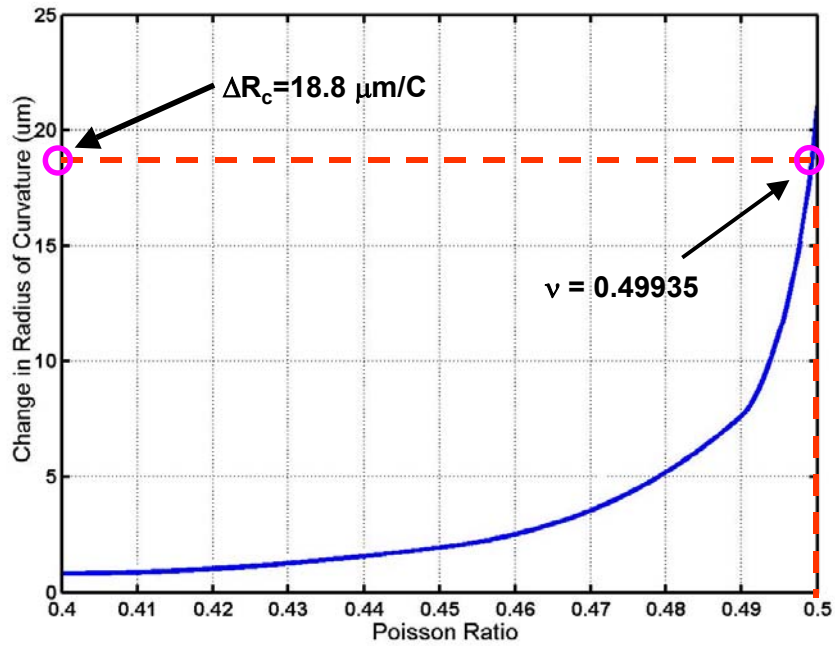


Figure 4. Radius of Curvature Change as a Function of RTV Poisson Ratio

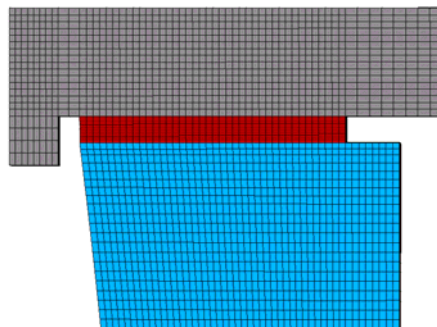


Figure 5. Design Trades Performed Using Simple Ring Bond Geometry

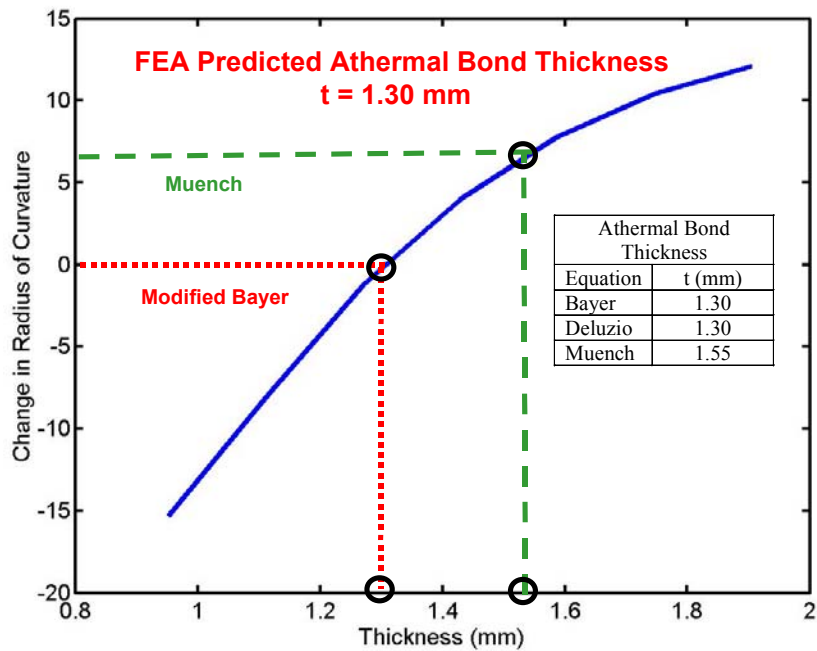


Figure 6. Change in the Radius of Curvature of the Primary Mirror as a Function of RTV Bond Thickness

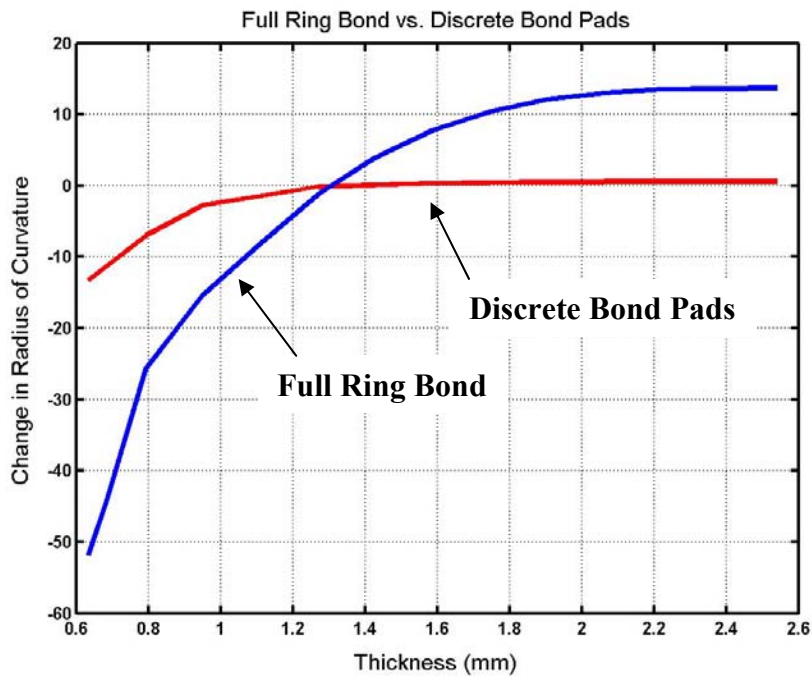


Figure 7. Change in the Radius of Curvature of the Primary Mirror as a Function of RTV Bond Thickness for Ring Bond and Discrete RTV Pads